

# RSC Advances



This is an *Accepted Manuscript*, which has been through the Royal Society of Chemistry peer review process and has been accepted for publication.

*Accepted Manuscripts* are published online shortly after acceptance, before technical editing, formatting and proof reading. Using this free service, authors can make their results available to the community, in citable form, before we publish the edited article. This *Accepted Manuscript* will be replaced by the edited, formatted and paginated article as soon as this is available.

You can find more information about *Accepted Manuscripts* in the [Information for Authors](#).

Please note that technical editing may introduce minor changes to the text and/or graphics, which may alter content. The journal's standard [Terms & Conditions](#) and the [Ethical guidelines](#) still apply. In no event shall the Royal Society of Chemistry be held responsible for any errors or omissions in this *Accepted Manuscript* or any consequences arising from the use of any information it contains.

# Molecular Insight and Resolution for Tumor Harbored H-ras(G12V) Mutation

Hsin-Chieh Tang<sup>a</sup> and Calvin Yu-Chian Chen<sup>\*a,b,c</sup>

<sup>a</sup> *Department of Biomedical Informatics, Asia University, Taichung, 41354, Taiwan*

<sup>b</sup> *Human Genetic Center, Department of Medical Research, China Medical University  
Hospital, Taichung, 40402, Taiwan*

<sup>c</sup> *Research Center for Chinese Medicine & Acupuncture, China Medical University,  
Taichung, 40402, Taiwan*

\*Corresponding author. Tel.: +886-4-22052121 ext. 4306

E-mail address: ycc929@MIT.EDU (C. Y.-C. Chen)

## Abstract

Recent study about physiological regulators of oncogenic growth has been published in the literature. When H-ras gene mutates, the mutant H-ras(G12V) protein causes uncontrolled cell growth. We tried to observe is there any difference of the wild type and mutant H-ras protein in the molecular character and structural variation *in silico*. Our hypothesis is H-ras(G12V) protein accompanied with altered structure might be responsible for excess signal transduction and even tumor formation. In this study, we wanted to find the potent compound that could bind to H-ras(G12V) protein and interfere the phosphorylation of substrate protein. By the methods of homology modeling, structure-based docking, candidate screening, and molecular dynamics (MD) simulation, we demonstrated that structural and molecular character of H-ras and H-ras(G12V) proteins were different. Abrine could bind to H-ras(G12V) and might interfere the phosphorylation process. These results provided a novel insight for the management of tumor or cancer which harbored H-ras(G12V) mutation.

**Keywords:** *in silico*; H-ras inhibitor; H-ras(G12V); traditional Chinese medicine (TCM); structure-based; molecular dynamics (MD) simulation

## Introduction

There is one study about physiological regulators of oncogenic growth.<sup>1</sup> H-ras protein receives growth factor stimulation and regulates cell division.<sup>2</sup> It is a GTPase involved in signal transduction pathways.<sup>3</sup> H-ras protein becomes active through binding with guanosine triphosphate (GTP).<sup>4</sup> Rapid response of cell proliferation can be induced by H-ras protein injection in animal experiment.<sup>5</sup> It is evident that H-ras plays a proto-oncogenic role in tumor formation.<sup>6</sup> When H-ras gene mutates, the mutant protein causes uncontrolled cell growth.<sup>7</sup> This mutation occurs in only one amino acid substitute of normal H-ras protein.<sup>8</sup> It replaces the normal amino acid glycine (G) with valine (V) at position 12 (known as G12V mutation).<sup>9</sup> The mutated H-ras protein is overactive even in the absence of outside growth factor stimulation.<sup>10</sup> Finally, it leads to endless cell proliferation and tumor formation.<sup>11</sup> In this study, we attempted to observe is there any difference of the normal and mutant H-ras(G12V) protein in structure-based docking procedure and molecular dynamics (MD) simulation.

H-ras gene is located at the position 15.5 on the short arm of chromosome 11. It belongs to the Ras superfamily of small GTPases. There are many proteins in the Ras superfamily. They attach to the cell membrane by the prenylation or palmitoylation domain.<sup>12</sup> Ras protein plays a switch on/off role in signal transduction.<sup>13</sup> It is in the "on" state while binding with GTP. After transduction of one phosphate group, it is in the "off" state while GTP transforms to guanosine diphosphate (GDP). So the Ras active or inactive state depends on the GTP-bound or GDP-bound form. Ras proteins are involved in transmitting external signal into the cells.<sup>14</sup> The signal pathway following Ras is rapidly accelerated fibrosarcoma / mitogen-activated protein kinase / extracellular signal-regulated kinase (RAF/MAPK/ERK) pathway. ERK controls cell division, proliferation and differentiation subsequently.<sup>15</sup>

"Ras" is referred to the abbreviation of "Rat sarcoma" which means its relationship to the oncogenes.<sup>16</sup> The well-known members in the superfamily are K-ras, N-ras and H-ras. The three Ras proteins share high sequence identities and similarities. All of them are associated with cell division, proliferation and differentiation.<sup>17</sup> They are the most common human Ras oncogenes leading to tumor formation.<sup>18</sup> Ras oncogenes are also related to tumor invasion and even metastasis.<sup>19</sup> Ras mutation is notorious for its oncogenic characteristic.<sup>20</sup> Thus, Ras inhibitors are one kind of choices to manage the tumor.<sup>21</sup> Scientists seek the way to inhibit Ras protein activity.<sup>22</sup> H-ras is a hot topic in physiological regulation of oncogenic growth. If we know the mechanism how H-ras protein transmits the signal, we can suppress tumor formation by blocking the signal pathway.<sup>23</sup> Accompanied with modern technology, the function of H-ras protein can be disrupted.<sup>24</sup> Tumor therapy for the target of other oncogenes may provide a new idea to inhibit the activity of mutant H-ras protein.<sup>25</sup>

As we know, the mutant H-ras protein can be responsible for tumor or cancer. Our hypothesis is mutant H-ras(G12V) protein accompanied with altered structure might lead to its oncogenic feather. In this study, we attempted to search the small molecular compound that may be H-ras(G12V) protein inhibitor. In other words, we wanted to find the compound that could bind to H-ras(G12V) protein successfully and interfere the contact of GTP and substrate protein. Thanks to modern technology, computer-aided drug design (CADD) saves our time to select appropriate drug compound rapidly compared with traditional one-by-one biochemistry.<sup>26, 27</sup> Structure-based methods employ docking procedure and MD simulation.<sup>28, 29</sup> Best candidate from docking and MD simulation can be selected as the potential therapeutic drug.<sup>30</sup> Traditional Chinese medicine (TCM) combines tradition and innovation together.<sup>31</sup> There are many advantages for utilizing TCM database to

conduct CADD.<sup>32</sup> Thus, we tried to utilize the largest TCM Database@Taiwan (<http://tcm.cmu.edu.tw/>) in the world to search the small molecular compound that has the ability to be H-ras(G12V) protein inhibitor for tumor suppression.<sup>33</sup>

## Materials and Methods

### Homology modeling

We obtained the sequence and 3D structure of human H-ras protein from the Uniprot Knowledgebase (P01112, human, 189 amino acids) and Protein Data Bank (PDB ID: 4Q21), respectively. We performed homology modeling of H-ras(G12V) protein by the Build Homology Models program in Accelrys Discovery Studio (DS) 2.5. We further confirmed the H-ras(G12V)-modeled structure by Ramachandran plot with Rampage program in DS 2.5.<sup>34</sup>

### Structure-based docking and candidate screening

We utilized the small molecular compounds from TCM Database@Taiwan to dock with H-ras(G12V) protein. Docking with target protein was the necessary step for the ligand to produce subsequent influence of binding forces and even structural change. It was important to estimate if any given ligand could match to the binding sites of target protein. We minimized all docking poses between the ligands and H-ras(G12V) protein by the force field of Chemistry at HARvard Molecular Mechanics (CHARMm).<sup>35</sup> LigandFit program in DS 2.5 was utilized to conduct docking procedure. The first step was to determine the binding sites of H-ras(G12V) protein. Key residues for the candidate's binding sites were set around GDP-bound sites. The second step was to generate the ligand's conformation by Monte Carlo method and dock with the binding sites. The third step is to calculate the binding affinity and binding scores between the ligand and H-ras(G12V) protein.<sup>36</sup> In this study, we adopted the scores of piecewise linear potentials (-PLP1 and -PLP2) to compare the

binding affinity for the TCM compounds and the control with H-ras(G12V) protein.<sup>37</sup>

### **Molecular dynamics (MD) simulation**

The procedure of molecular binding was a dynamic process. To count and analyze the data of the dynamic process, we needed a method for mathematical calculation. The package of Groningen MACHine for Chemical Simulations (GROMACS) program was utilized for MD simulation. The assumed four phases for each ligand-protein complex were minimization, heating, equilibration, and finally, production. The cytoplasmic situation was set as transferable intermolecular potential 3P (TIP3P) water with 0.9% sodium chloride concentration. The minimization course comprised 500 steps of steepest descent and conjugated gradient. The heating course comprised 50K to 310K within 50 picoseconds (ps). The equilibration course comprised 310K for 150 ps. The production course comprised constant temperature for 20 nanoseconds (ns). The trajectories of root mean square deviation (RMSD), mean square displacement (MSD), solvent accessible surface area (SASA), radius of gyration (Rg) and total energy were illustrated to discover the secret of MD simulation. We drew the diagrams of root mean square fluctuation (RMSF) to compare the change of individual residues. Cluster analysis and the representative structure, docking and molecular MD snapshots were illustrated to compare the differences of H-ras, H-ras(G12V) and abrine.<sup>38,39</sup>

## **Results and Discussion**

### **Homology modeling**

We substituted the amino acid glycine (G) with valine (V) at position 12 in the sequence of H-ras protein, and constructed H-ras(G12V)-modeled structure according to the wild type template (4Q21, human H-ras protein). Ramachandran plot of

H-ras(G12V)-modeled structure demonstrated that 94.6% of residues were in the favored region, 4.2% were in the allowed region, only 1.2% were in the outlier region (Fig. 1).

We chose human H-ras(G12V) protein sequence and human H-ras template (4Q21) as the homologous model to construct the ideal H-ras(G12V)-modeled structure. By analyzing Ramachandran plot, the high percentage of residues in the favored (94.6%) and allowed (4.2%) regions implied that the H-ras(G12V)-modeled structure was a reasonable conformational model.

### **Structure-based docking and candidate screening**

We utilized GDP as the ligand-binding control model of H-ras and H-ras(G12V) protein. GDP was the compound existed in the crystal complex of 4Q21 recruited by the Protein Data Bank, too. Table 1 listed piecewise linear potential (PLP) scores of top 9 candidates screening from TCM Database@Taiwan. Based on the docking result, we chose abrine as the candidate for further investigation (Fig. 2). The binding residues between GDP and H-ras or H-ras(G12V) protein were illustrated. GDP formed hydrogen bond (H-bond) with Gly13, Lys16, Ser17, Ala18 and Lys117 of H-ras protein. GDP formed H-bond with Gly13, Gly15, Lys16 and Lys117 of H-ras(G12V) protein. Abrine formed H-bond with Lys117 and Asp119 of H-ras(G12V) protein (Fig. 3).

Comparison of GDP-bound H-ras and H-ras(G12V) protein, there were common and different binding residues. Gly13, Lys16 and Lys117 were their common binding residues by docking procedure. Gly15, Ser17 and Ala18 were their different binding residues. It was evident that even the tiny change (G12V) could induce slight different binding results. Further comparison of GDP-bound and abrine-bound H-ras(G12V) protein, Lys117 was their only common binding residue. It was evident that abrine bound to H-ras(G12V) protein near the GDP binding sites. This result speculated that

abrine might interfere the contact of GTP and substrate protein.

### **Molecular dynamics (MD) simulation**

#### **Molecular character**

First, we focused on two conditions of molecular character in the period of MD. One was wild type GDP-bound H-ras and mutant H-ras(G12V) protein, the other was abrine and GDP-bound H-ras(G12V) protein.

The trajectory of root mean square deviation (RMSD) was drawn to evaluate the deviation degree of each ligand and its relevant H-ras or H-ras(G12V) protein. H-ras had the highest average protein RMSD value. In contrast, the relevant protein of abrine had the lowest average protein RMSD value. Interestingly, abrine had the highest average ligand RMSD value among the three ligands. H-ras was higher than H-ras(G12V), too (Fig. 4). It was evident that GDP or its relevant H-ras(G12V) protein was more stable than wild type H-ras protein. This result speculated that GTP-bound H-ras(G12V) provided a more stable condition to phosphorylate the substrate protein.

We drew the trajectory of mean square displacement (MSD) to investigate the molecular deviation distance of each ligand and its relevant protein. H-ras had the highest average protein MSD value. In contrast, the relevant protein of abrine had the lowest average protein MSD value. Interestingly, abrine had the highest ligand MSD value among the three ligands. Average value of H-ras was higher than H-ras(G12V), too (Fig. 5). It was evident that although abrine has certain degree deviation, its relevant protein was quite stable. This result speculated that abrine might interfere the contact of GTP and substrate protein.

The trajectory of solvent accessible surface area (SASA) was drawn to evaluate water contact surface of each ligand and its relevant protein. H-ras had the highest average protein SASA value. In contrast, H-ras(G12V) had the lowest average protein

SASA value (Fig. 6). However, the average ligand SASA value of abrine was extremely higher than H-ras or H-ras(G12V). We supposed this result might reflect that abrine molecule had long hydrophobic tail (Fig. 7).

We drew the trajectory of radius of gyration (Rg) to investigate the degree of compactness of each ligand and its relevant protein. H-ras had the highest average protein Rg value among the three proteins. However, abrine had the highest average ligand Rg value, and H-ras(G12V) had the lowest average value (Fig. 8). It was evident that GDP or its relevant H-ras(G12V) protein was more compact than wild type H-ras protein. This result speculated that GTP-bound H-ras(G12V) provided a closer condition to phosphorylate the substrate protein.

The trajectory of total energy was drawn to evaluate the binding energy needed for each ligand and its relevant protein. The frequent total energy for H-ras, H-ras(G12V) and abrine was around -415500, -415500 and -409000 kJ/mol, respectively (Fig. 9). According to the trajectories of total energy, abrine was higher than H-ras and H-ras(G12V). We supposed that single mutation of H-ras protein didn't affect its binding stability with GDP, but abrine might bind to H-ras(G12V) successfully with higher energy.

### **Structural variation**

In the following section, we focused on the comparison of detailed structural or conformational variation of these three protein: H-ras, H-ras(G12V) and the relevant H-ras(G12V) protein for abrine.

We showed the diagram of root mean square fluctuation (RMSF) to assess the fluctuation degree from the view of every residue. All of the three protein had similar RMSF pattern, but the number matrix could tell us the difference. The highest relative value was 1 which meant no difference. The relative value between H-ras and H-ras(G12V) was 0.5476. The relative values of between abrine and H-ras(G12V) or

H-ras were 0.7919 and 0.795 (Fig. 10). Based on the relative value of RMSF number matrix between H-ras and H-ras(G12V), it was evident that there was certain degree of structural change even due to single mutation. It was in accordance with our hypothesis that mutant H-ras(G12V) protein was accompanied with altered structure.

We performed cluster analysis to determine the representative structure of each ligand and its relevant protein in the period of MD. The time for representative structure of H-ras, H-ras(G12V) and abrine was 15.06, 15.96 and 13.44 ns, respectively. GDP formed H-bond with Val14, Gly15, Lys16, Ser17 and Lys117 of H-ras protein at 15.06 ns. GDP formed H-bond with Gly15, Lys16 and Ser17 of H-ras(G12V) protein at 15.96 ns. Abrine formed H-bond with Lys117 of H-ras(G12V) protein at 13.44 ns (Fig. 11).

Comparative diagrams of docking and MD snapshot for H-ras, H-ras(G12V) and abrine were illustrated. We adopted overlapping methods to display the difference of docking and MD snapshot for the ligand and its relevant protein. H-bond and hydrophobic contact were important binding forces for the connection between the ligand and its relevant protein. The binding angles of abrine changed prominently. Besides the binding angles, there was one prominent difference of docking and MD snapshot for H-ras(G12V) protein. The important binding residue Lys117 which existed in docking was lost at 15.96 ns of MD (Fig. 15-17).

Based on cluster analysis and comparative diagrams of docking and MD snapshot, there were several important findings. Except the binding angles, there was no prominent change for H-ras protein. However, the important binding residue Lys117 which existed in docking was lost at 15.96 ns of MD for H-ras(G12V) protein. It was evident that H-ras(G12V) lost Lys117 connection gradually due to conformational change during MD. This change provided abrine a chance to bind with H-ras(G12V) protein and the changing binding angles might interfere the contact

of GTP and substrate protein.

## Conclusion

By the results of MD simulation, such as RMSD, MSD, SASA, Rg and RMSF, H-ras(G12V) had different molecular character and structural variation from wild type H-ras protein. We also demonstrated that altered structure might provide a more convenient condition to phosphorylate the substrate protein. According to structure-based docking, candidate screening, and MD simulation, it was evident that abrine might interfere the contact of GTP and substrate protein. Above findings provided a novel idea or insight for management of tumor or cancer which harbored H-ras(G12V) mutation.

## Acknowledgements

The research was supported by grants from China Medical University Hospital (DMR-103-096). The study is supported in part by Taiwan Ministry of Health and Welfare Clinical Trial and Research Center of Excellence (MOHW104-TDU-B-212-113002), and CMU under the Aim for Top University Plan of the Ministry of Education, Taiwan, too.

## References

1. S. Beronja, P. Janki, E. Heller, W. H. Lien, B. E. Keyes, N. Oshimori and E. Fuchs, *Nature*, 2013, 501, 185-190.
2. K. Irani, Y. Xia, J. L. Zweier, S. J. Sollott, C. J. Der, E. R. Fearon, M. Sundaresan, T. Finkel and P. J. Goldschmidt-Clermont, *Science*, 1997, 275, 1649-1652.
3. J. C. Lacal, P. de la Pena, J. Moscat, P. Garcia-Barreno, P. S. Anderson and S.

- A. Aaronson, *Science*, 1987, 238, 533-536.
4. I. A. Prior, A. Harding, J. Yan, J. Sluimer, R. G. Parton and J. F. Hancock, *Nat Cell Biol*, 2001, 3, 368-375.
  5. C. Collin, A. G. Papageorge, D. R. Lowy and D. L. Alkon, *Science*, 1990, 250, 1743-1745.
  6. J. R. Feramisco, M. Gross, T. Kamata, M. Rosenberg and R. W. Sweet, *Cell*, 1984, 38, 109-117.
  7. U. Krengel, I. Schlichting, A. Scherer, R. Schumann, M. Frech, J. John, W. Kabsch, E. F. Pai and A. Wittinghofer, *Cell*, 1990, 62, 539-548.
  8. D. Meder and K. Simons, *Science*, 2005, 307, 1731-1733.
  9. Y. Wakabayashi, J. H. Mao, K. Brown, M. Girardi and A. Balmain, *Nature*, 2007, 445, 761-765.
  10. A. Goriely, R. M. Hansen, I. B. Taylor, I. A. Olesen, G. K. Jacobsen, S. J. McGowan, S. P. Pfeifer, G. A. McVean, E. Rajpert-De Meyts and A. O. Wilkie, *Nat Genet*, 2009, 41, 1247-1252.
  11. S. A. Radkov, P. Kellam and C. Boshoff, *Nat Med*, 2000, 6, 1121-1127.
  12. J. F. Hancock, H. Paterson and C. J. Marshall, *Cell*, 1990, 63, 133-139.
  13. O. Rocks, A. Peyker, M. Kahms, P. J. Verveer, C. Koerner, M. Lumbierres, J. Kuhlmann, H. Waldmann, A. Wittinghofer and P. I. Bastiaens, *Science*, 2005, 307, 1746-1752.
  14. H. Schipper, E. A. Turley and M. Baum, *Lancet*, 1996, 348, 1149-1151.
  15. M. Malumbres and M. Barbacid, *Nat Rev Cancer*, 2003, 3, 459-465.
  16. D. Bar-Sagi and J. R. Feramisco, *Science*, 1986, 233, 1061-1068.
  17. M. A. White, C. Nicolette, A. Minden, A. Polverino, L. Van Aelst, M. Karin and M. H. Wigler, *Cell*, 1995, 80, 533-541.
  18. K. H. Vahakangas, J. M. Samet, R. A. Metcalf, J. A. Welsh, W. P. Bennett, D. P.

- Lane and C. C. Harris, *Lancet*, 1992, 339, 576-580.
19. N. Hayashi, I. Ito, A. Yanagisawa, Y. Kato, S. Nakamori, S. Imaoka, H. Watanabe, M. Ogawa and Y. Nakamura, *Lancet*, 1995, 345, 1257-1259.
20. M. Oft, R. J. Akhurst and A. Balmain, *Nat Cell Biol*, 2002, 4, 487-494.
21. J. Chen and R. Iyengar, *Science*, 1994, 263, 1278-1281.
22. S. M. Johnson, H. Grosshans, J. Shingara, M. Byrom, R. Jarvis, A. Cheng, E. Labourier, K. L. Reinert, D. Brown and F. J. Slack, *Cell*, 2005, 120, 635-647.
23. M. H. Tsai, C. L. Yu and D. W. Stacey, *Science*, 1990, 250, 982-985.
24. S. Roy, R. Luetterforst, A. Harding, A. Apolloni, M. Etheridge, E. Stang, B. Rolls, J. F. Hancock and R. G. Parton, *Nat Cell Biol*, 1999, 1, 98-105.
25. F. Su, A. Viros, C. Milagre, K. Trunzer, G. Bollag, O. Spleiss, J. S. Reis-Filho, X. Kong, R. C. Koya, K. T. Flaherty, P. B. Chapman, M. J. Kim, R. Hayward, M. Martin, H. Yang, Q. Wang, H. Hilton, J. S. Hang, J. Noe, M. Lambros, F. Geyer, N. Dhomen, I. Niculescu-Duvaz, A. Zambon, D. Niculescu-Duvaz, N. Preece, L. Robert, N. J. Otte, S. Mok, D. Kee, Y. Ma, C. Zhang, G. Habets, E. A. Burton, B. Wong, H. Nguyen, M. Kockx, L. Andries, B. Lestini, K. B. Nolop, R. J. Lee, A. K. Joe, J. L. Troy, R. Gonzalez, T. E. Hutson, I. Puzanov, B. Chmielowski, C. J. Springer, G. A. McArthur, J. A. Sosman, R. S. Lo, A. Ribas and R. Marais, *N Engl J Med*, 2012, 366, 207-215.
26. X. Y. Pan, H. Guo, J. Han, F. Hao, Y. An, Y. Xu, Y. Xiaokaiti, Y. Pan and X. J. Li, *Eur J Pharmacol*, 2012, 683, 27-34.
27. H. C. Tang and C. Y. Chen, *Evid Based Complement Alternat Med*, 2014, 2014, 254678.
28. S. Tian, J. Wang, Y. Li, X. Xu and T. Hou, *Mol Pharm*, 2012, 9, 2875-2886.
29. H. C. Tang and C. Y. Chen, *Evid Based Complement Alternat Med*, 2014, 2014, 385120.

30. H. C. Tang and C. Y. Chen, *Biomed Res Int*, 2014, 2014, 798742.
31. Z. Li, Y. Liu, L. Wang, X. Liu, Q. Chang, Z. Guo, Y. Liao, R. Pan and T. P. Fan, *Evid Based Complement Alternat Med*, 2014, 2014, 392324.
32. H. C. Tang and C. Y. Chen, *Evid Based Complement Alternat Med*, 2014, 2014, 928589.
33. C. Y. Chen, *PLoS One*, 2011, 6, e15939.
34. C. Y. Chen, *Curr Top Med Chem*, 2013, 13, 965-988.
35. K. Vanommeslaeghe, E. Hatcher, C. Acharya, S. Kundu, S. Zhong, J. Shim, E. Darian, O. Guvench, P. Lopes, I. Vorobyov and A. D. Mackerell, Jr., *J Comput Chem*, 2010, 31, 671-690.
36. M. Montes, M. A. Miteva and B. O. Villoutreix, *Proteins*, 2007, 68, 712-725.
37. C. Y. Chen, *J Biomol Struct Dyn*, 2009, 27, 271-282.
38. D. Van Der Spoel, E. Lindahl, B. Hess, G. Groenhof, A. E. Mark and H. J. Berendsen, *J Comput Chem*, 2005, 26, 1701-1718.
39. S. Pronk, S. Pall, R. Schulz, P. Larsson, P. Bjelkmar, R. Apostolov, M. R. Shirts, J. C. Smith, P. M. Kasson, D. van der Spoel, B. Hess and E. Lindahl, *Bioinformatics*, 2013, 29, 845-854.

**Table 1** Piecewise Linear Potential (PLP) scores of top 10 candidates screening from TCM Database@Taiwan.

Name	-PLP1	-PLP2
Abrine	65.01	63.57
Saussureamine A	59.55	57.98
N-Methyl tyramine-O-alpha-L-rhamnopyranoside	29.36	34.53
3_4_5-trimethoxy_benzeneethanamine	28.6	26.2
Mescaline	27.7	23.87
Norerythrostachaldine	23.17	20.15
(S)-cathinone	12.07	6.91
Norephedrine	14.03	14.29
Hexyl amine-1	13.6	8.48
Guanosine-5'-Diphosphate*	51.31	55.4

## Figure Legends

**Fig. 1** Ramachandran plot of H-ras(G12V)-modeled structure. Number of residues in favored region (~98.0% expected) : 157 (94.6%). Number of residues in allowed region (~2.0% expected) : 7 (4.2%). Number of residues in outlier region : 2 (1.2%).

**Fig. 2** Scaffold of the ligands. (A) Guanosine diphosphate (GDP) for H-ras protein. (B) GDP for H-ras(G12V) protein. (C) Abrine for H-ras(G12V) protein.

**Fig. 3** Schematic diagram of the binding area for the ligand and (A) H-ras protein, and (B) H-ras(G12V) protein. Docking poses of the ligand and its corresponding protein: (C) GDP-bound H-ras, (D) GDP-bound H-ras(G12V), and (E) abrine-bound H-ras(G12V).

**Fig. 4** Root mean square deviation for (A) protein RMSD, and (B) ligand RMSD.

**Fig. 5** Mean square displacement for (A) protein MSD, and (B) ligand MSD.

**Fig. 6** Solvent accessible surface area (protein SASA) for (A) GDP corresponding H-ras, (B) GDP corresponding H-ras(G12V), and (C) abrine corresponding H-ras(G12V).

**Fig. 7** Solvent accessible surface area (ligand SASA) of (A) GDP for H-ras, (B) GDP for H-ras(G12V), and (C) abrine for H-ras(G12V).

**Fig. 8** Radius of gyration (Rg) for (A) protein, and (B) ligand.

**Fig. 9** Total energy for (A) GDP-bound H-ras, (B) GDP-bound H-ras(G12V), and (C) abrine-bound H-ras(G12V).

**Fig. 10** (A) The trajectories of root mean square fluctuation (RMSF). (B) The matrix of RMSF for H-ras, H-ras(G12V) and abrine.

**Fig. 11** Cluster analysis and the representative structure for (A) GDP-bound H-ras, (B) GDP-bound H-ras(G12V), and (C) abrine-bound H-ras(G12V).

**Fig. 12** Comparative diagrams of docking and molecular dynamics (MD) snapshot for GDP bound with H-ras protein.

**Fig. 13** Comparative diagrams of docking and molecular MD snapshot for GDP bound with H-ras(G12V) protein.

**Fig. 14** Comparative diagrams of docking and MD snapshot for abrine bound with H-ras(G12V) protein.

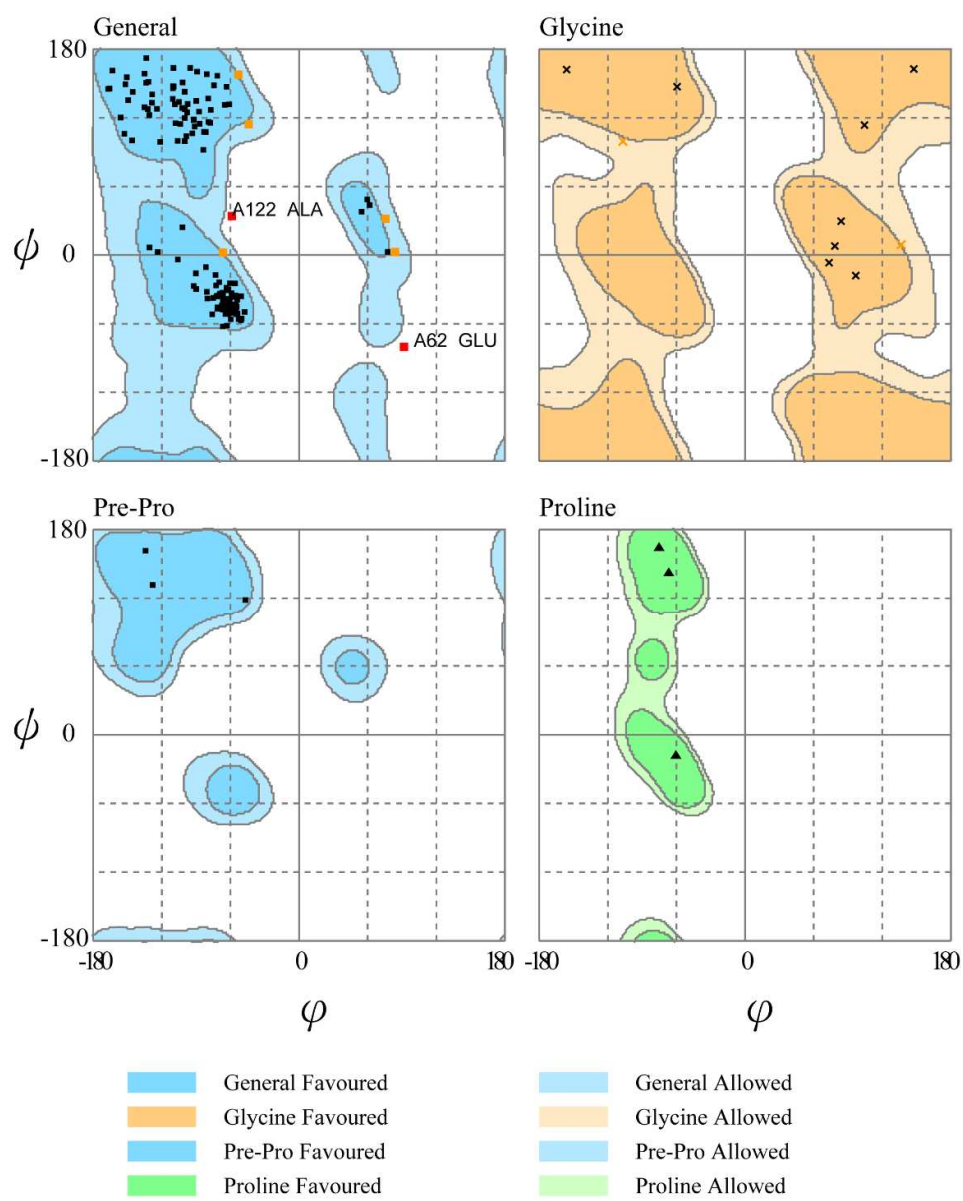


Fig. 1

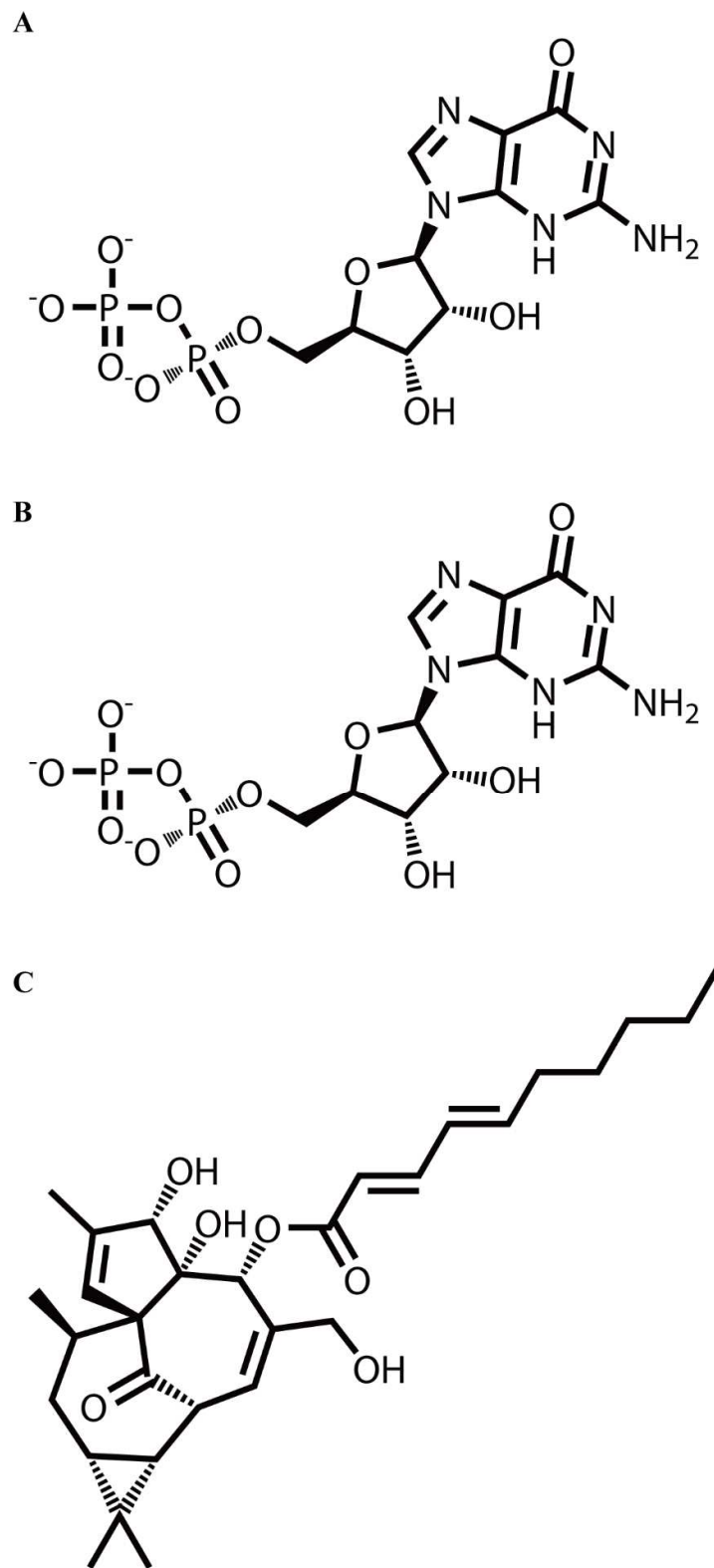


Fig. 2

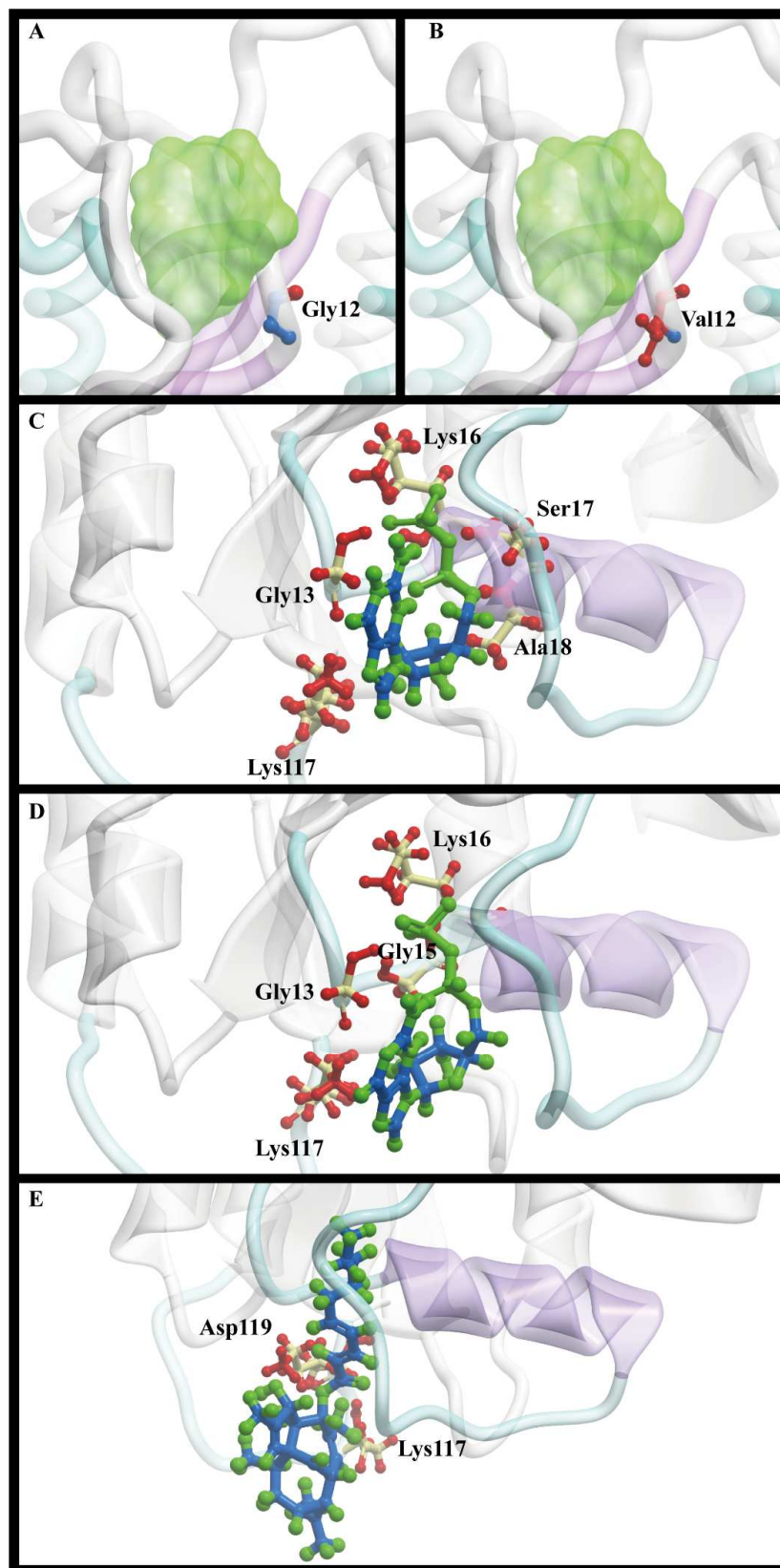


Fig. 3

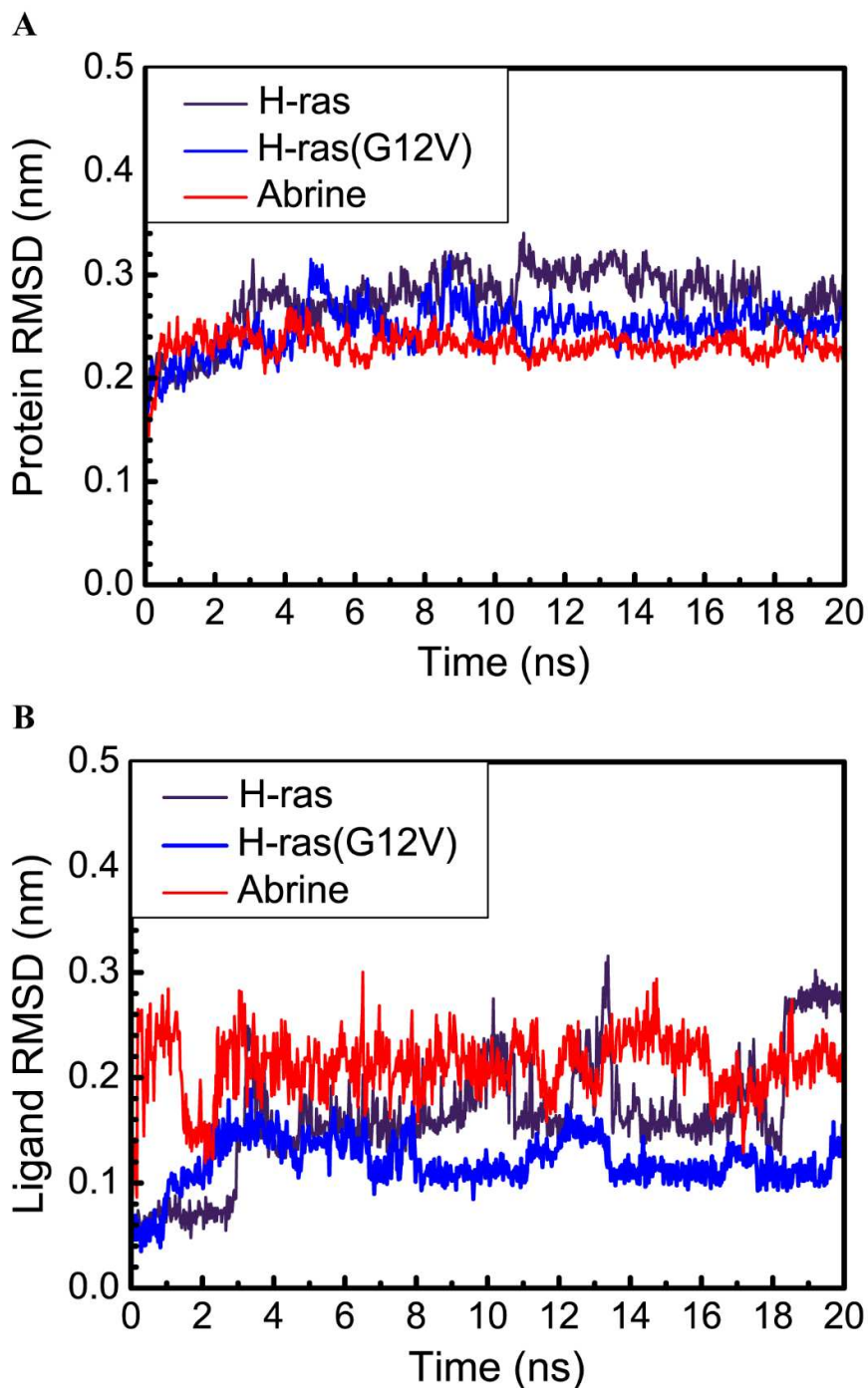


Fig. 4

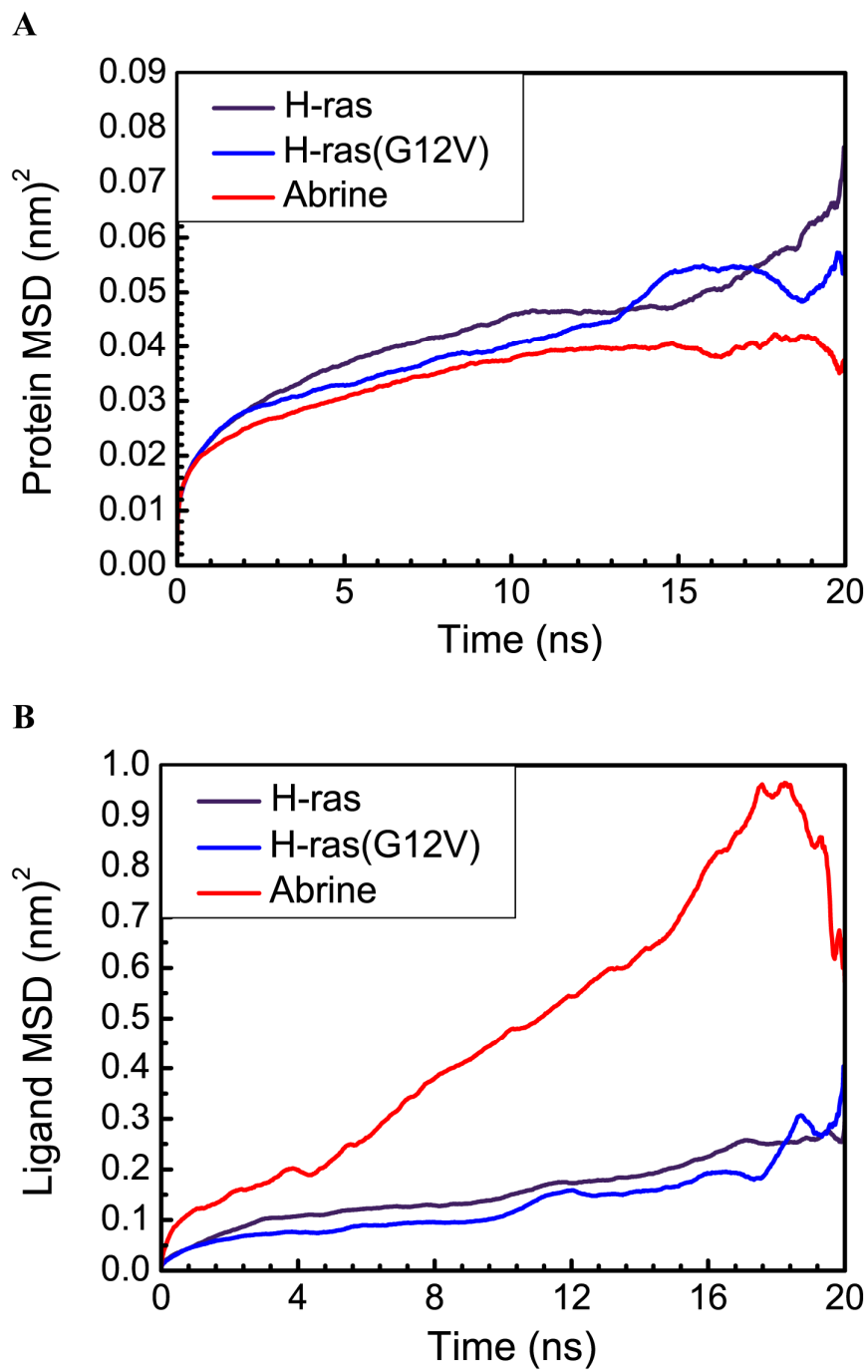


Fig. 5

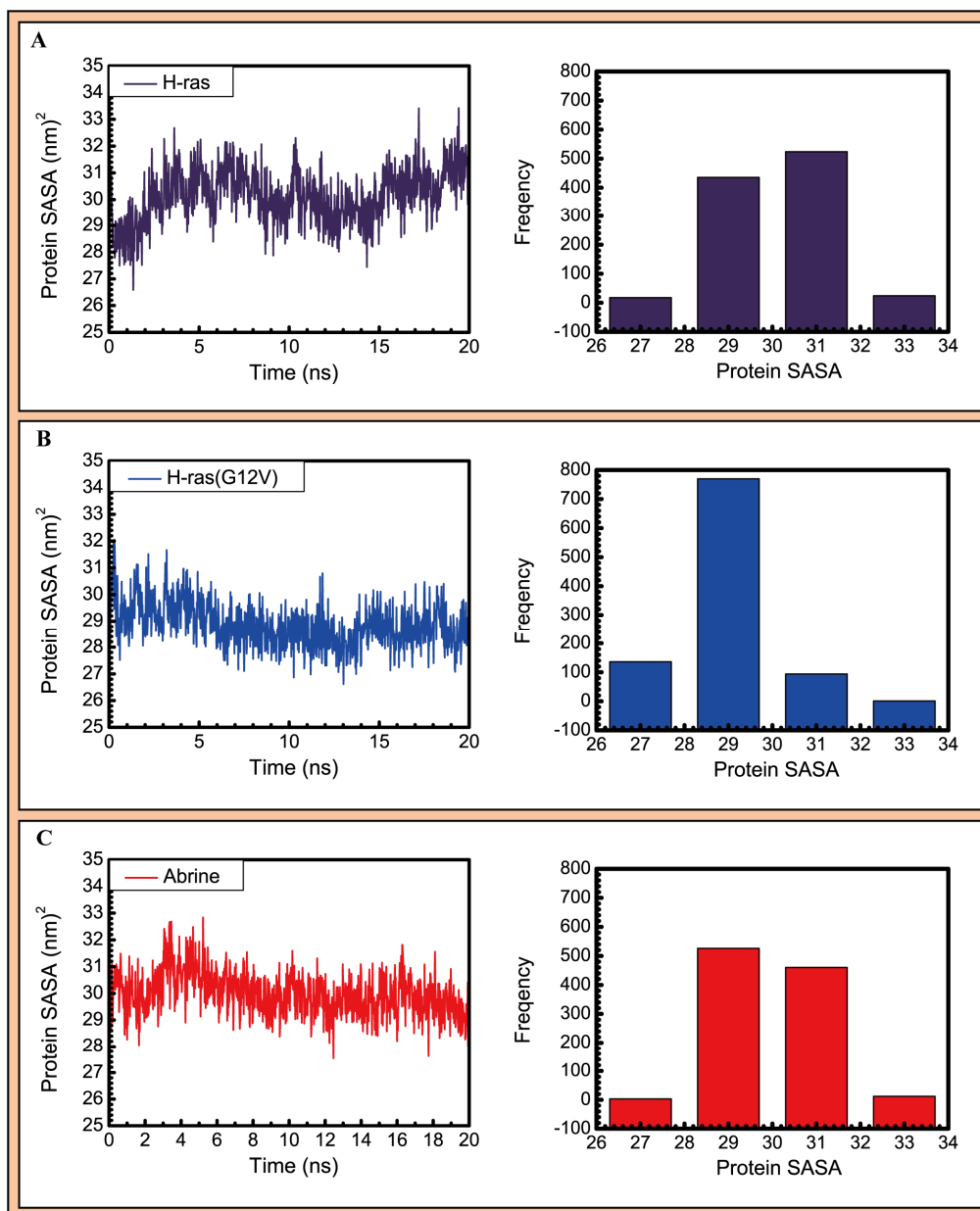


Fig. 6

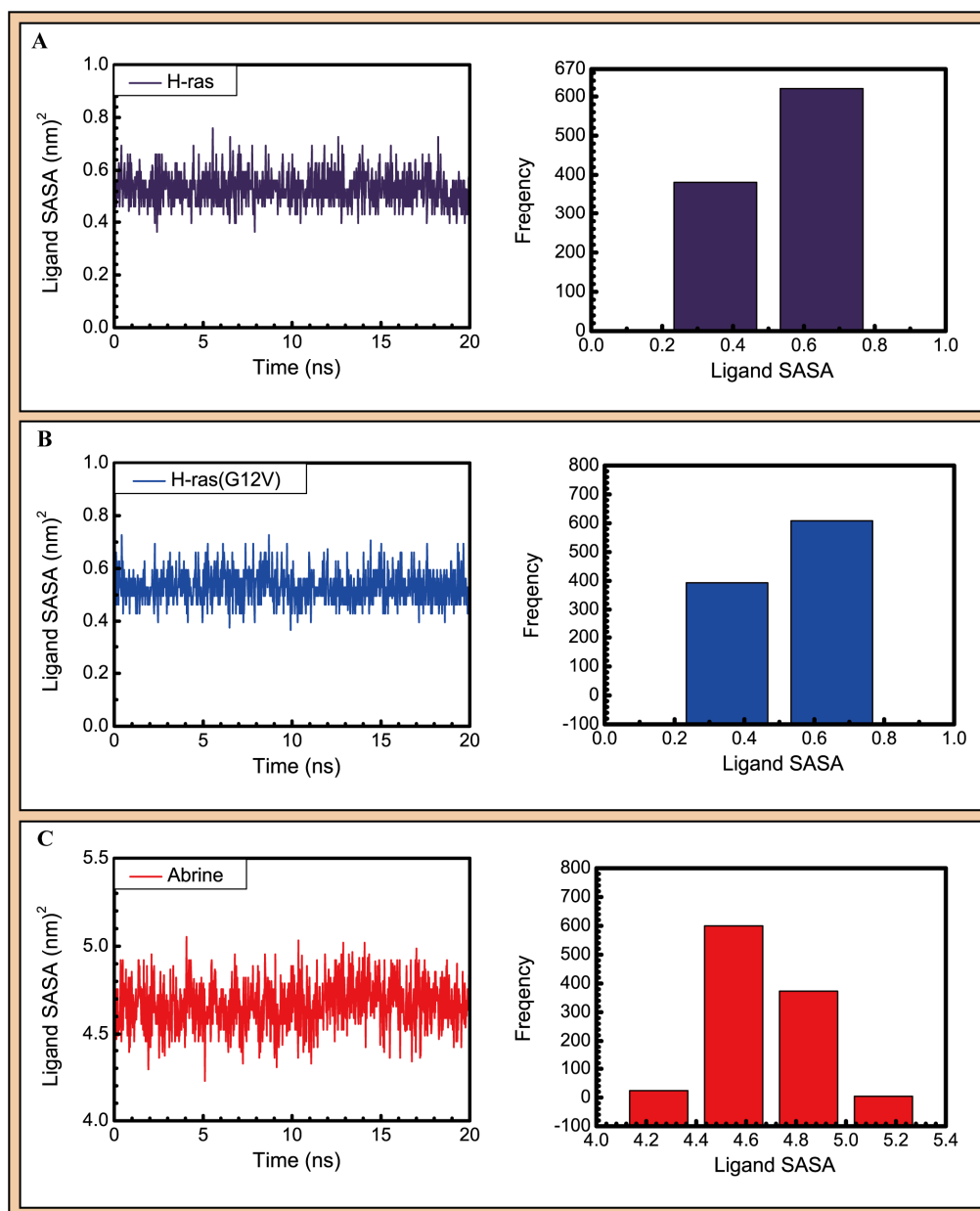


Fig. 7

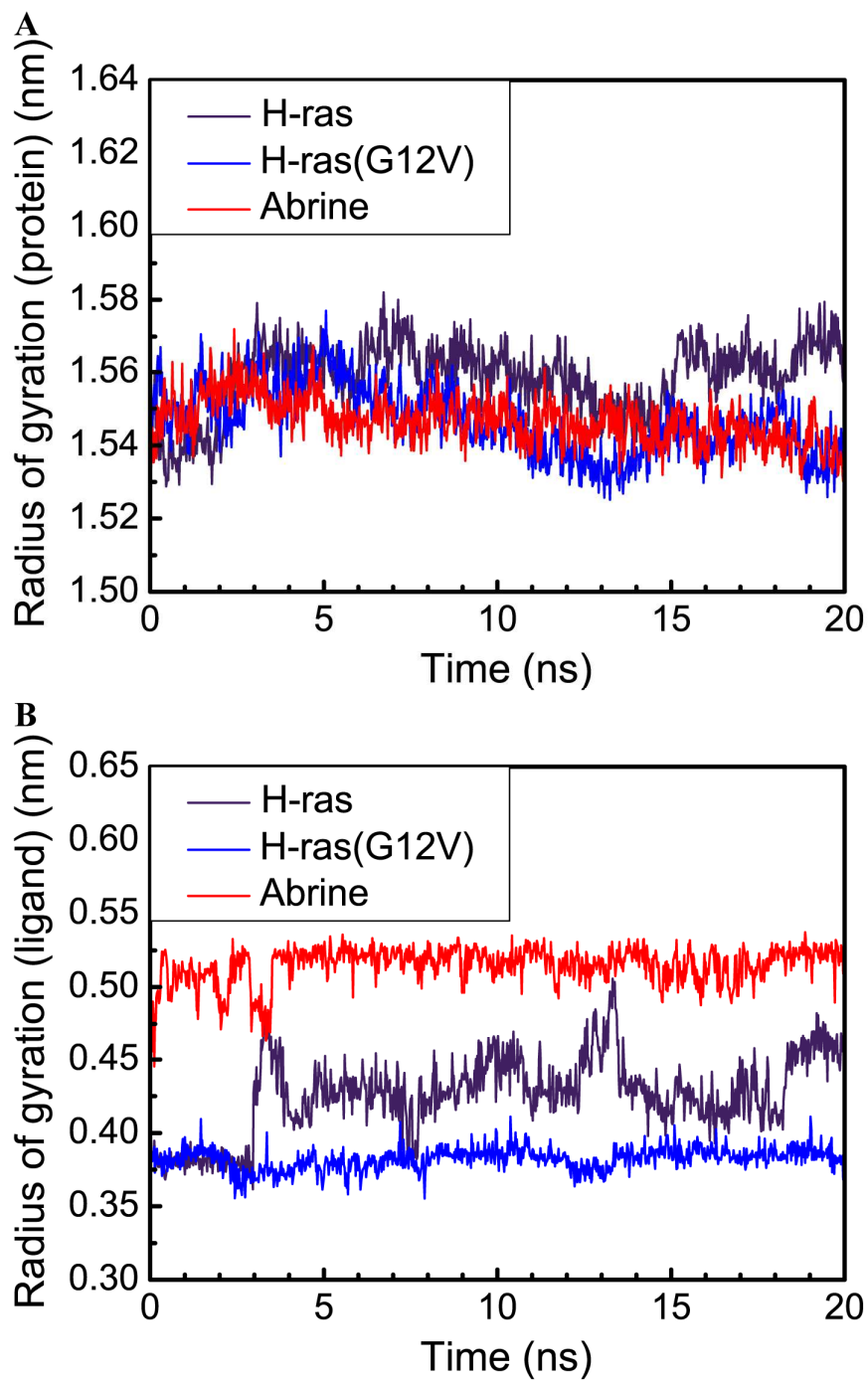


Fig. 8

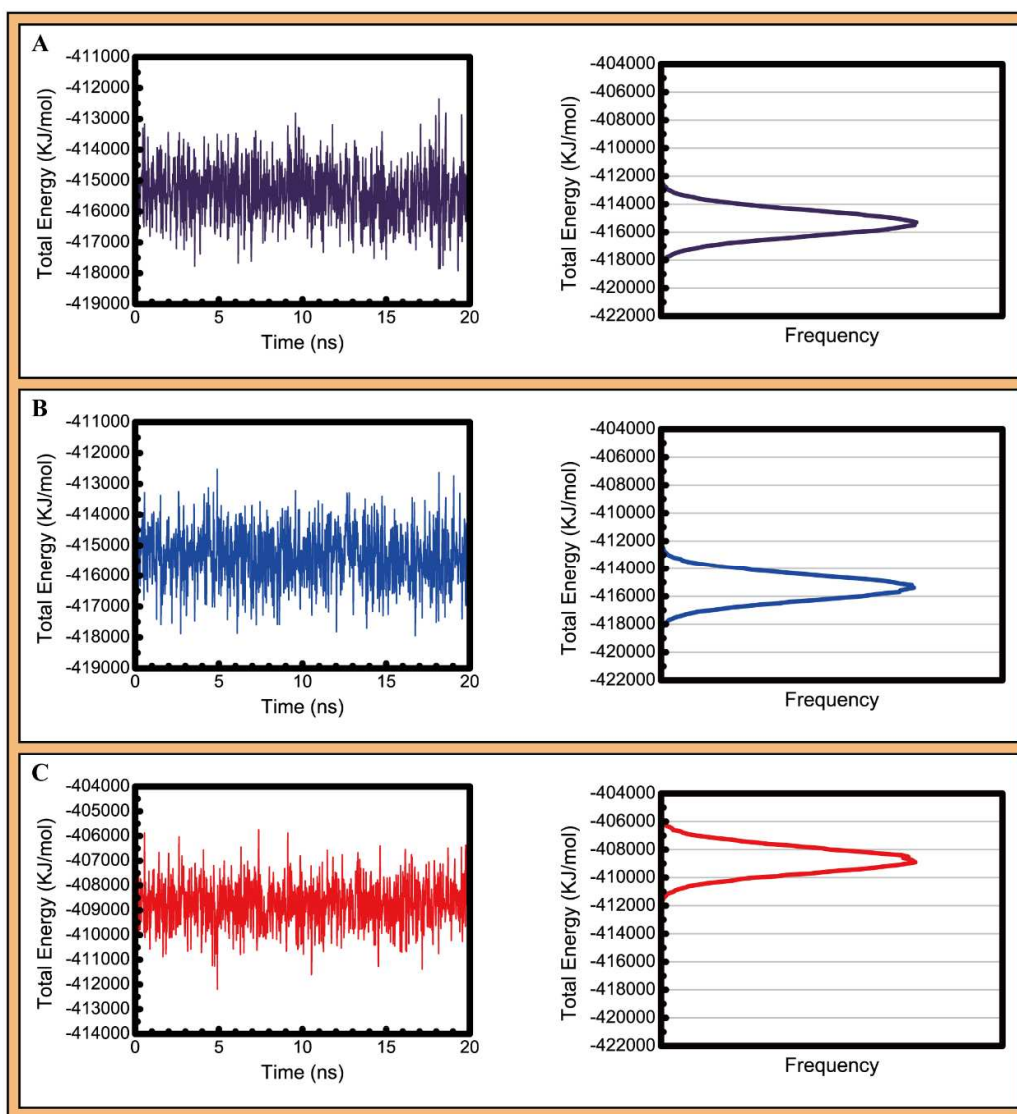


Fig. 9

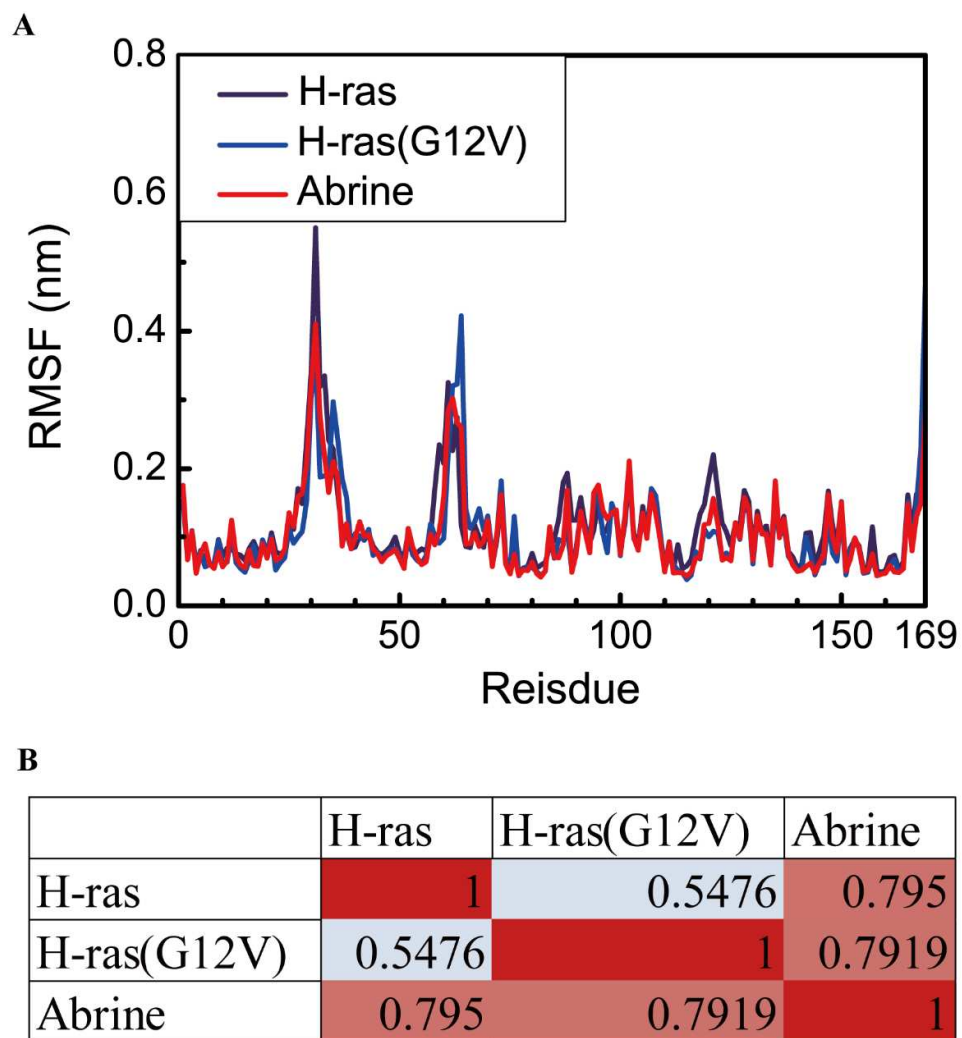


Fig. 10

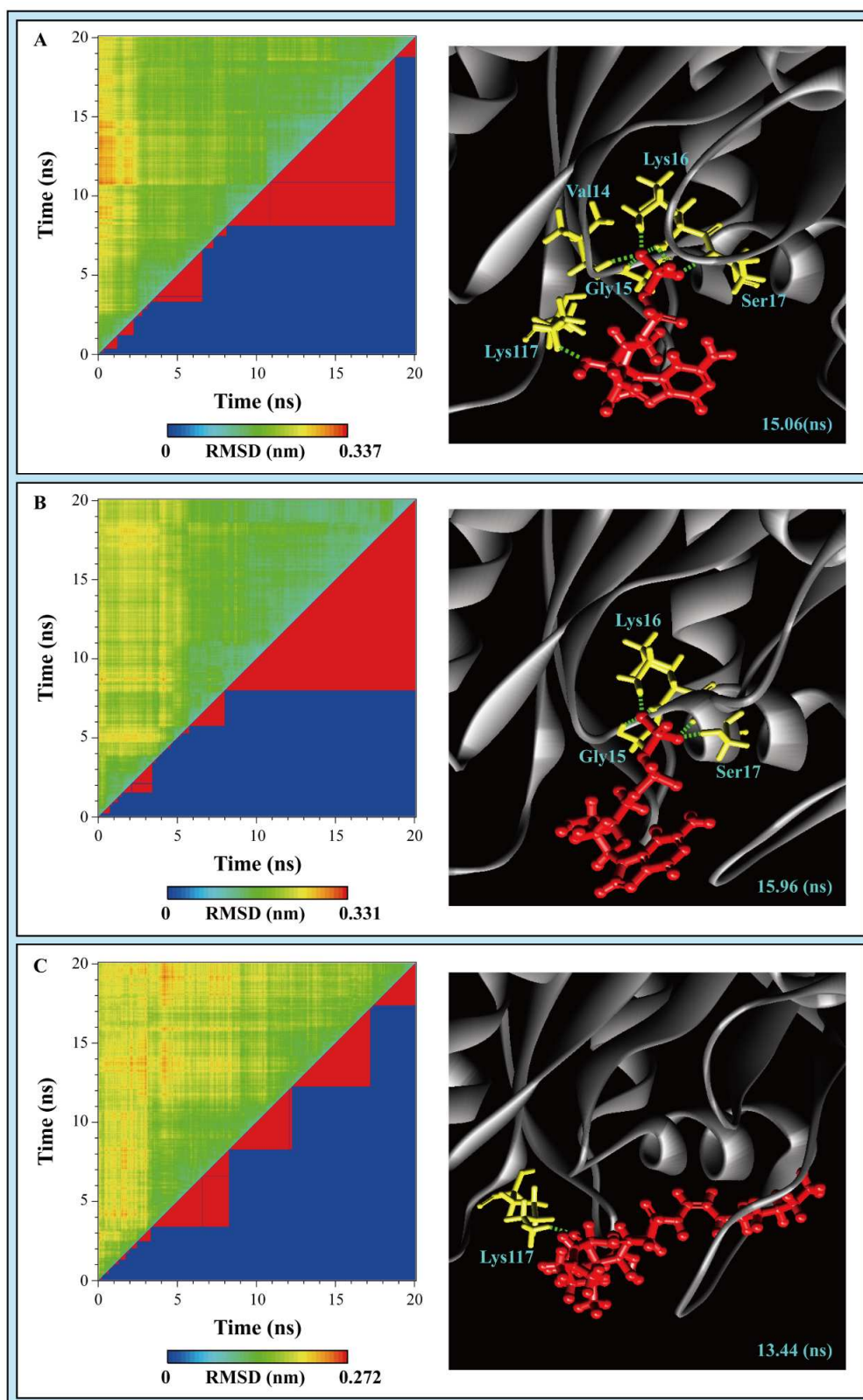


Fig. 11



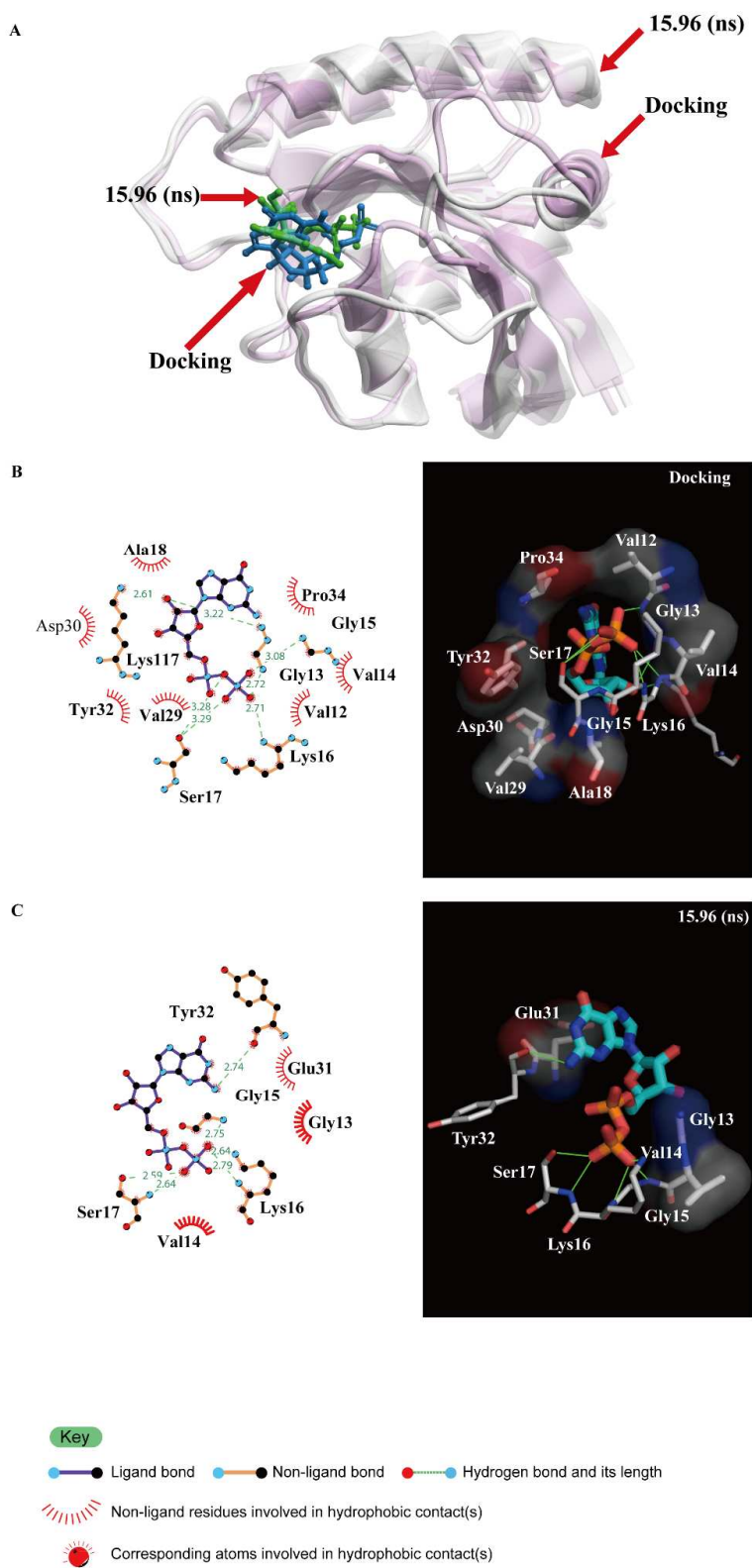
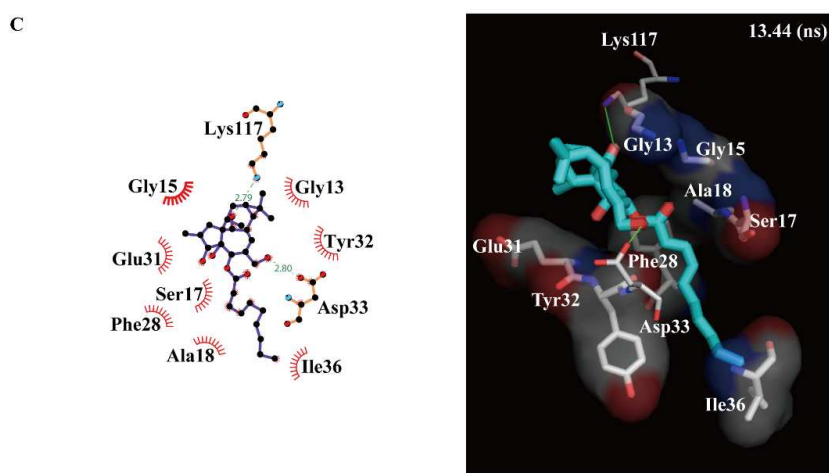
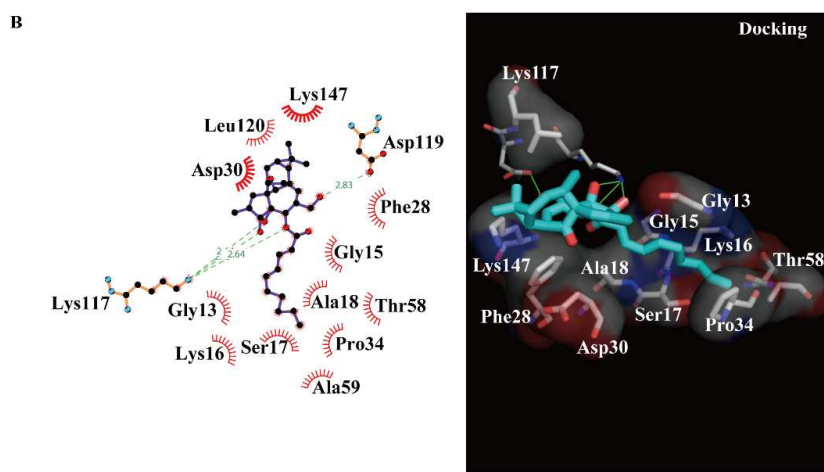
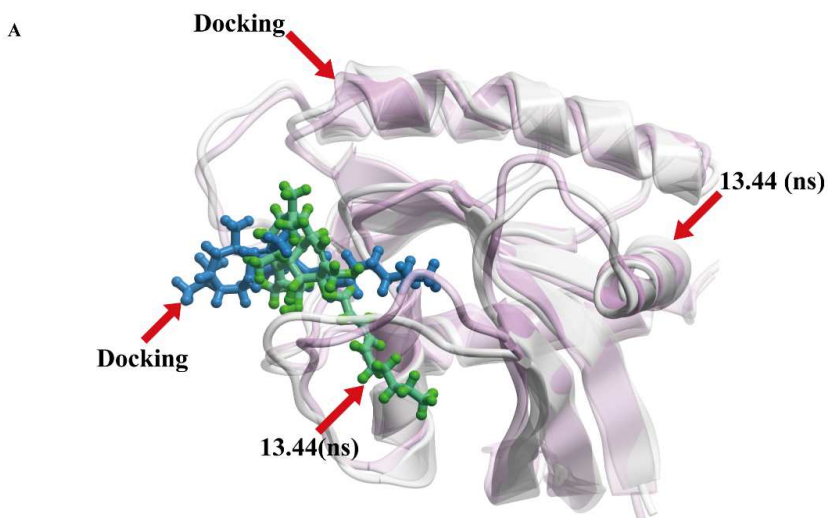


Fig. 13



Key

●—● Ligand bond   ●—● Non-ligand bond   ●—● Hydrogen bond and its length

⋯ Non-ligand residues involved in hydrophobic contact(s)

⋯ Corresponding atoms involved in hydrophobic contact(s)

**Fig. 14**